MgO melting curve constraints from shock temperature and rarefaction overtake measurements in samples preheated to 2300 K

2014 J. Phys.: Conf. Ser. 500 062003

(http://iopscience.iop.org/1742-6596/500/6/062003)

Journal of Physics: Conference Series **500** (2014) 062003 doi:10.1088/1742-6596/500/6/062003

MgO melting curve constraints from shock temperature and rarefaction overtake measurements in samples preheated to 2300 K

O V Fat′yanov[1] and P D Asimow[2]

Division of Geological and Planetary Sciences 170-25, California Institute of Technology, Pasadena, CA 91125, USA

E-mail: [1]fatyan1@gps.caltech.edu, [2]asimow@gps.caltech.edu

Abstract. Continuing our effort to obtain experimental constraints on the melting curve of MgO at 100-200 GPa, we extended our target preheating capability to 2300 K. Our new Mo capsule design holds a long MgO crystal in a controlled thermal gradient until impact by a Ta flyer launched at up to 7.5 km/s on the Caltech two-stage light-gas gun. Radiative shock temperatures and rarefaction overtake times were measured simultaneously by a 6-channel VIS/NIR pyrometer with 3 ns time resolution. The majority of our experiments showed smooth monotonic increases in MgO sound speed and shock temperature with pressure from 197 to 243 GPa. The measured temperatures as well as the slopes of the pressure dependences for both temperature and sound speed were in good agreement with those calculated numerically for the solid phase at our peak shock compression conditions. Most observed sound speeds, however, were ~800 m/s higher than those predicted by the model. A single unconfirmed data point at 239 GPa showed anomalously low temperature and sound speed, which could both be explained by partial melting in this experiment and could suggest that the Hugoniot of MgO preheated to 2300 K crosses its melting line just slightly above 240 GPa.

1. Introduction

The phase relations and thermodynamic properties of MgO at high pressure, ~100-200 GPa, are important in several disciplines including geophysics, geochemistry, and planetary science. Despite considerable theoretical [1–5] and experimental [6–8] effort, however, the melting behavior of MgO in this pressure range still remains essentially unknown, as is clear from the wide range of relevant results from the scientific literature shown in figure 1.

Zerr and Boehler [6] reported experimental data on pure MgO melting in a laser-heated diamond anvil cell to 31.5 GPa and an extrapolation of the melting curve to 135 GPa using the Lindemann relation. The melting slope of MgO at 1 bar from their measurements is 36 K/GPa. Zhang and Fei [7] determined the melting behavior of (Mg,Fe)O ferropericlase to 7 GPa in a resistively heated multi-anvil apparatus together with compositional extrapolation to the pure MgO end member. Their estimate for the melting slope of pure MgO at 1 bar is 221 K/GPa. We have been addressing this issue with a campaign of shock temperature measurements in preheated <100> single crystal MgO.

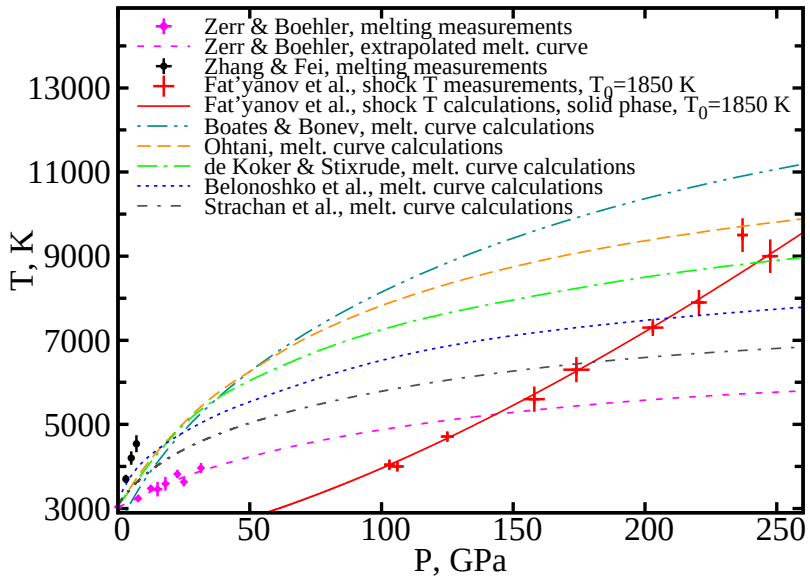

Figure 1. Pressure - temperature diagram of MgO to 250 GPa showing the melting data from [1–7] and our unpublished true-temperature data measured along the 1850 K Hugoniot. All crosses indicate the actual error bars.

Preliminary quasi-brightness temperature data on the 1850 K Hugoniot at shock pressures up to 203 GPa were reported in Fat′yanov et al. [8]; extension of these data to higher pressure and unpublished final true-temperature data place a lower bound for the melting curve of ~9000 K at 240 GPa. The results of numerous calculations, including ones not shown in figure 1, yield initial slopes in the range of 88 to 150 K/GPa [9–12] and predict MgO melting temperature at the Earth's core-mantle boundary pressure, ~135 GPa, from 6000 to 9000 K.

In order to reach the intercept of a hot Hugoniot with the melting line, we have successfully developed the whole experimental technique to enable measurements on samples preheated to 2300 K. Although this initial temperature is only 450 K higher than that in the previous series [8], this turned out to be the practical limit given available materials, facilities, and resources.

2. Experimental Approach and Procedure

The technique described here has successfully addressed two serious engineering challenges. First, MgO undergoes intense sublimation and even thermal decomposition when heated above ~2000 K in vacuum [13, 14]. Its hot surfaces rapidly lose optical polish, scatter light passing through them, and preclude quantitative absolute intensity measurements of light emitted from shocked material within the crystal. Second, intense heat fluxes and substantial flows of evaporated materials from such hot targets significantly degrade the properties of nearby optical components and introduce systematic wavelength-dependent errors in radiative temperature measurements due to light scattering in free space and on mirror and lens surfaces.

Our most recent experimental configuration is shown schematically in figure 2. The target is a single crystal of >99.95% pure MgO, 12 mm square by 20.2 mm thick, with one <100> face optically polished (Red Optronics), suspended on 4 pieces of 50 μm thick, 99.95% pure W foil (Alpha Aesar) inside a two-piece threaded assembly of >99.97% pure Mo (H. C. Starck Inc. ABL-1.75 rod specification). The first part forms a 4 mm thick driver plate inside a 15 mm inner diameter sample chamber. Four 5 mm diameter ventilation holes prevented vapor pressure build-up and formation of bubbles at the polished MgO free surface. The second part is a 22 mm outer diameter cap with an 11.5 mm diameter opening at the center for the outgoing light intensity measurements. A disk of 25 μm thick, 99.98% pure W foil (ESPI metals) as well as a pinhole-free, 13 μm thick, 99.8% pure Ti foil (Alpha Aesar) are stacked between the Mo driver plate and the MgO crystal. The heating coil is placed such

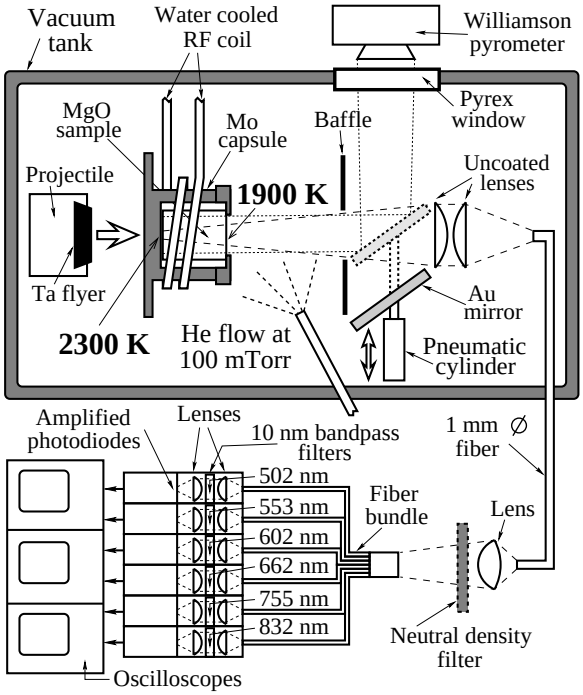

Figure 2. Schematic of the most recent experimental configuration in firing position.

that the end of the MgO crystal in contact with the driver plate is the hottest part, with temperature decreasing by ~400 K towards the optically polished (downrange) free surface of the MgO crystal. This allows viewing of shock temperature in MgO heated to 2300 K near the driver surface through the relatively cold surface of the MgO without issues of evaporation or scattering. The W foil was necessary to reach 2300 K. We were unable to heat above ~2100 K when the MgO was in direct contact with hot Mo.

A pair of N-BK7 uncoated plano-convex lenses (250 mm focal length, $f/3.33$, Edmund Optics Inc) formed a ~1.5x demagnified image of the target on a 1 mm diameter, 0.39 N/A multimode fiber patch cord (Thorlabs Inc). The other end of the fiber was imaged by a 20 mm diameter, $f/1$ biconvex, AR-coated relay lens onto the 5 mm diameter common end tip of a 6-branch custom multiple fiber bundle (Oriel Corp). The rest of the 6-channel pyrometer design and setup was nearly identical to that described in [8]. Absolute intensity calibration used a N.I.S.T.-traceable spectral radiance source (Optronic Laboratories, Inc., W ribbon lamp model 550G). Initial temperature of MgO crystal near the Mo driver plate was measured to ±50 K by a 710/810 nm Williamson pyrometer (model PRO 81-70-C-FOV15IN/150).

The first 3 experiments at 2300 K initial temperature were done using the extendable turning mirror configuration described in [8], without He purge. However, post-shot tests in the gun tank during which the mirror was extended towards the hot target for ~1 second, revealed significant – roughly 10 to 30% – decrease of turning mirror reflectivity at all wavelengths. Therefore, for subsequent experiments we developed an optical fiber configuration (figure 2). The majority of these shots employed a He purge in the proximity of the hot target. The purpose of the He flow is to reduce pressure of evaporated target materials and to carry solid particles streaming off the hot target assembly out of the optical path to the pyrometer. No difference in gun performance or recorded radiative shock temperatures at 550-830 nm wavelengths was noticed between the experiments with and without He purge.

3. Data Analysis

The previous configuration that we used for shock temperature study in MgO preheated up to 1850 K also yielded shock velocity measurements [8], whereas the new configuration instead yields measurements of the sound speed in the shock state from rarefaction overtake time. Another essential difference is that the high-impedance W foil needed to reach the highest temperatures creates a reverberation that leads to multiple-shock, rather than single-shock, compression. In all our 2300 K experiments, the first pressure jump is ~85% of the peak value, followed by a few reverberations to the final state. This compression path is less favorable for high temperature generation than a single shock wave. For the same final shock pressure, corresponding peak temperature is ~600-800 K lower than that on the 2300 K single-shock Hugoniot.

The shock states in the samples were calculated from projectile velocities measured to 0.1-0.2% uncertainty, the known Hugoniot for cold Ta [15], and Hugoniot parameters extrapolated to higher temperatures for Mo (1673 K) [16], W (298 K) [17], and MgO (1850 K) [8]. Thicknesses and initial densities of hot Mo, W, and MgO were recalculated from ambient values using reported thermal expansion data and measured target temperatures [8]. All Hugoniot parameters are summarized in table 1.

Representative spectral radiance data from two shots done in the fiber configuration with He purge are shown in figures 3 and 4. The shock wave in each case enters the MgO at time 0 ns and gets overtaken by a well-defined rarefaction originating from the back of Ta flyer, observed simultaneously on all 6 pyrometer channels at the times shown. For sound speed analysis in the compressed state of MgO we compared the measured rarefaction overtake times with ones predicted by the one-dimensional finite-difference wave propagation code WONDY V [18], using material models that assume γ/V=constant and the reported ambient values of Grüneisen coefficients for Ta, Mo, and W and the room-temperature value of 1.4 for MgO fitted to our temperature measurements along the 1850 K Hugoniot (table 1).

Quasi-brightness shock temperatures for the estimated lower limit of shock front reflectivity of 2% were extracted for each pyrometer channel [8]. The results listed in figures 3 and 4 show reasonably good agreement between these temperatures measured at different wavelengths.

The assumed true temperatures for all 2300 K experiments were obtained from observed quasi-brightness temperatures using an estimated 18% shock front reflectivity. This is the average value measured for MgO shock compressed to 220 and 248 GPa in our previous series of experiments at 1850 K initial temperature. These experiments were designed to measure shock front reflectivity using a ~50/50 normal-incidence, high-temperature beamsplitter constructed from a stack of five spaced 0.25 mm thick sapphire windows. The principle is to compare observed light intensity in a matched pair of experiments at the same initial temperature and roughly the same projectile velocity, with and without the beamsplitter [19]. For a non-reflecting shock front, the intensity received at the pyrometer in the experiment with the beamsplitter will just be the intensity in the non-beamsplitter experiment reduced by the external transmittance of the beamsplitter. Any light reflected backwards by the beamsplitter will be completely absorbed by shock-compressed material (multiple Fresnel reflections at the MgO-vacuum interface are not discussed here for simplicity but are accounted for in our experimental data analysis). However, for a reflecting shock-front there will be additional intensity due to multiply-reflected light (reflected backwards by beamsplitter, reflected forwards by shock-front, transmitted through the beam splitter on the second pass, next fraction reflected backwards by beamsplitter, and so on). The simplified relationship between the shock front reflectivity, r, and the light intensities recorded in experiments without and with the beamsplitter, respectively I_0 and I_1, is

$$r = (1 - \frac{I_0}{I_1}T)/R, \tag{1}$$

where T is the external transmittance and R is the reflectance of the beamsplitter for incoherent unpolarized light.

Table 1. Equation of state parameters for the materials we used. C and S are linear Hugoniot coefficients that relate shock velocity, U_s, and particle velocity, U_p, as $U_s = C + S \cdot U_p$.

Material	Initial Density, ρ_0 (g/cm^3)	C (km/s)	S	Grunëisen γ at ρ_0
cold Ta	16.69	3.293	1.307	1.65
hot Mo	9.79	4.858	1.288	1.59
hot W	18.64	3.937	1.259	1.60
hot MgO	3.27	6.081	1.352	1.53

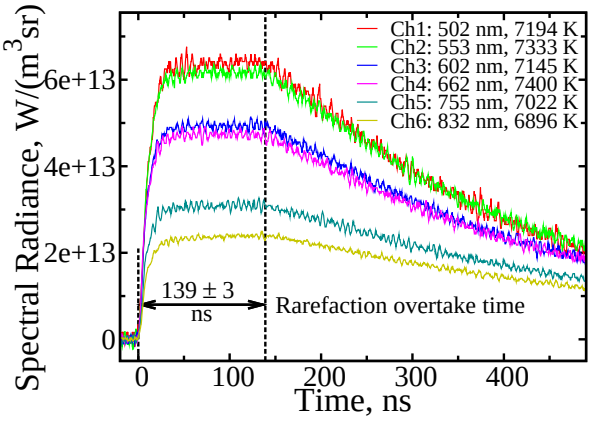

Figure 3. Spectral radiance histories from shot #490 at 197±4 GPa.

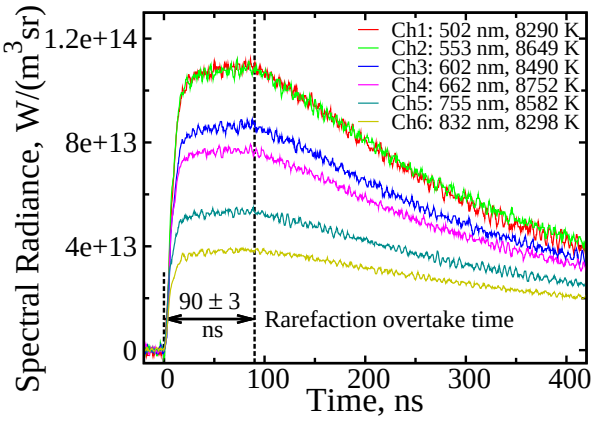

Figure 4. Spectral radiance histories from shot #487 at 243±4 GPa.

4. Summary and Conclusions

Preliminary results of our sound speed and temperature measurements in shock-compressed MgO at ~2300 K initial temperature are shown in figures 5 and 6; 3 mirror configuration (squares) and 6 fiber configuration (circles) experiments are plotted. Figure 5 shows that most sound speed values are about 800 m/s higher than expected. Since the sound speed for hot Mo is not accurately known, we cannot tell whether this discrepancy is caused by any systematic experimental errors or simply by inaccurate model predictions for hot Mo. Nevertheless, all the data except perhaps the single shot at 239 GPa are consistent with Birch′s Law (a linear relation between sound speed and volume [20]) for a single solid phase, with the correct slope.

All mirror configuration experiments showed temperatures at 436 nm about ~2000 K lower and at 502 nm ~500 K lower than the remaining channels at 553-755 nm. This pronounced spectral dependence was an experimental artifact caused by a UV absorption band in hot MgO and higher light scattering at shorter wavelengths by particles in the optical path of the 6-channel pyrometer. For these experiments, figure 6 shows shock temperatures computed as average values from 5 channels, 502 to 755 nm. They are lower than the model predictions even after applying a correction for 18% reflectivity of the shock front measured in 1850 K experiments in a similar pressure range.

All data points collected in the fiber configuration (figure 2) showed good agreement between the shock temperatures measured by 6 pyrometer channels from 502 to 832 nm. As shown in figure 6, radiative temperatures from these shots, corrected for 18% shock front reflectivity, agree quite well with the model predictions for B1 solid phase MgO in the shock state.

The highest pressure data point at 243±4 GPa showed slightly lower temperature than that predicted which may be an indication of partial melting. Another (mirror configuration) data point at 239±4 GPa gave anomalously low sound speed and temperature results. Although absolute light intensity values for this shot were not accurately recorded due to uncharacterized degradation of the turning mirror, the decrease in apparent temperature compared to lower pressure experiments with the same mirror configuration, together with the low sound speed observed in the same shot can be most easily explained by partial melting.

In conclusion, data reported here showed no evidence of MgO melting up to 232±4 GPa and 8800 K. Some features that may be explained by partial melting became noticeable at ~240 GPa and ~9000 K. Assuming no superheating, our new data exclude values of the 1 bar slope of the melting curve less than about 100 K/GPa and are most consistent with the melting curves calculated by Liu et al. [11] and by de Koker and Stixrude [4].

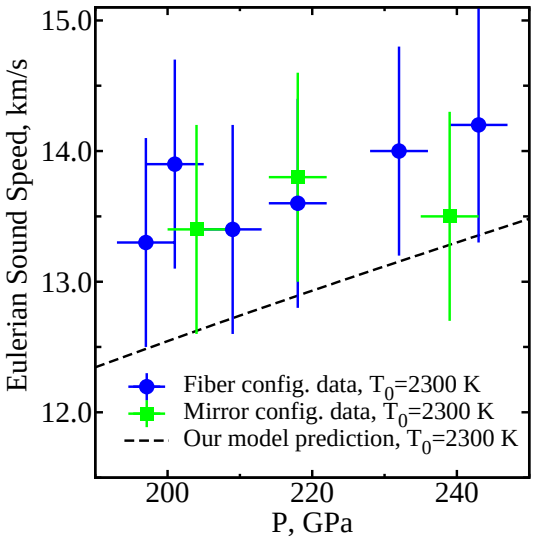

Figure 5. Summary of MgO sound speed data versus our model predictions. Crosses are the actual error bars.

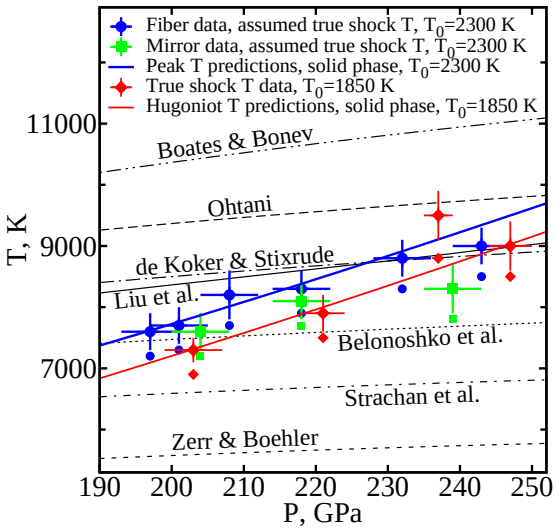

Figure 6. Summary of our shock temperature data and the melting curves from [1–6, 11]. Crosses are the actual error bars, smaller symbols show the measured quasi-brightness temperatures.

Acknowledgments

We are grateful to the late Prof. Thomas J. Ahrens for his deep interest and enthusiastic support of this research to the last days of his life. We thank M. Long, E. Gelle, and R. Oliver for technical help with our experiments. OVF thanks his newborn son Vladimir for the opportunity to finish writing and to submit this manuscript. Funded by NSF awards EAR-1119522 and EAR-1050269.

References

[1] Ohtani E 1983 *Phys. Earth Planet. In.* **33** 12-25
[2] Strachan A, Çağin T and Goddard III W A 1999 *Phys. Rev.* B **60** 15084-93
[3] Belonoshko A B, Arapan S, Martonak R and Rosengren A 2010 *Phys. Rev.* B **81** 054110
[4] de Koker N and Stixrude L 2009 *Geophys. J. Int.* **178** 162-79
[5] Boates B and Bonev S A 2013 *Phys. Rev. Lett.* **110** 135504
[6] Zerr A and Boehler R 1994 *Nature* **371** 506-8
[7] Zhang L and Fei Y 2008 *Geophys. Res. Lett.* **35** L13302
[8] Fat′yanov O V, Asimow P D and Ahrens T J 2009 *AIP Conf. Proc.* **1195** 855-8
[9] Cohen R E and Weitz J S 1998 *Geoph. Monog. Series* **101** 185-96
[10] Alfè 2005 *Phys. Rev. Lett.* **94** 235701
[11] Liu Z J, Sun X W, Chen Q F, Cai L C, Tan X M and Yang X D 2006 *Phys. Lett.* A **353** 221-5
[12] Tangney P and Scandolo S 2009 *J. Chem. Phys.* **131** 124510
[13] Lamoreaux R H, Hildenbrand D L and Brewer L 1987 *J. Phys. Chem. Ref. Data* **16** 419-43
[14] Ronchi C and Sheindlin M 2001 *J. Appl. Phys.* **90** 3325-31
[15] Mitchell A C and Nellis W J 1981 *J. Appl. Phys.* **52** 3363-74
[16] Asimow P D, Sun D and Ahrens T J 2009 *Phys. Earth Planet. In.* **174** 302-8
[17] Marsh S P 1980 *LANL shock Hugoniot data* (Berkeley, CA: University of California) 145-6
[18] Kipp M E and Lawrence R J 1982 WONDY V - a one-dimensional finite-difference wave propagation code *Sandia National Laboratories Tech. Rep.* SAND81-0930
[19] Fat′yanov O V, Ogura T, Nicol M F, Nakamura K G and Kondo K 2001 *Appl. Phys. Lett.* **77** 960-2
[20] Birch F 1961 *Geophys. J. Roy. Astr. S.* **4** 295-311